Essential role for mast cell tryptase in acute experimental colitis

Matthew J. Hamilton[a,b,1], Mark J. Sinnamon[a,b], Gregory D. Lyng[c], Jonathan N. Glickman[b,d], Xueli Wang[a,b], Wei Xing[a,b], Steven A. Krilis[e,f], Richard S. Blumberg[a,b], Roberto Adachi[g], David M. Lee[a,b], and Richard L. Stevens[a,b]

Departments of [a]Medicine and [d]Pathology, Harvard Medical School, Boston, MA 02115; [b]Brigham and Women's Hospital, Boston, MA 02115; [c]Biomodels, LLC, Watertown, MA 02472; [e]Department of Medicine, University of New South Wales, Sydney, NSW 2217, Australia; [f]Department of Immunology, Allergy, and Infectious Diseases, St. George Hospital, Sydney, NSW 2217, Australia; and [g]Department of Pulmonary Medicine, University of Texas M. D. Anderson Cancer Center, Houston, TX 77030

Edited by Warren Strober, National Institute of Allergy and Infectious Diseases, Bethesda, MD, and accepted by the Editorial Board November 29, 2010 (received for review April 28, 2010)

Patients with inflammatory bowel disease (IBD) have increased numbers of human tryptase-β (hTryptase-β)-positive mast cells (MCs) in the gastrointestinal tract. The amino acid sequence of mouse mast cell protease (mMCP)-6 is most similar to that of hTryptase-β. We therefore hypothesized that this mMCP, or the related tryptase mMCP-7, might have a prominent proinflammatory role in experimental colitis. The dextran sodium sulfate (DSS) and trinitrobenzene sulfonic acid (TNBS) colitis models were used to evaluate the differences between C57BL/6 (B6) mouse lines that differ in their expression of mMCP-6 and mMCP-7 with regard to weight loss, colon histopathology, and endoscopy scores. Microarray analyses were performed, and confirmatory real-time PCR, ELISA, and/or immunohistochemical analyses were carried out on a number of differentially expressed cytokines, chemokines, and matrix metalloproteinases (MMPs). The mMCP-6–null mice that had been exposed to DSS had significantly less weight loss as well as significantly lower pathology and endoscopy scores than similarly treated mMCP-6–expressing mice. This difference in colitis severity was confirmed endoscopically in the TNBS-treated mice. Evaluation of the distal colon segments revealed that numerous proinflammatory cytokines, chemokines that preferentially attract neutrophils, and MMPs that participate in the remodeling of the ECM were all markedly increased in the colons of DSS-treated WT mice relative to untreated WT mice and DSS-treated mMCP-6–null mice. Collectively, our data show that mMCP-6 (but not mMCP-7) is an essential MC-restricted mediator in chemically induced colitis and that this tryptase acts upstream of many of the factors implicated in IBD.

When activated via their pathogen-recognition, complement, purinergic, or Ig receptors, mast cells (MCs) release substantial amounts of numerous biologically active factors to carry out their beneficial functions in innate and adaptive immunity. Among the preformed granule mediators that are highly restricted to these tissue-residing immune cells in mice are the two closely related tryptases, mouse MC protease (mMCP)-6 and mMCP-7 (1–3). These two serine proteases reside in the cell's granules ionically bound to serglycin proteoglycans as homotypic and heterotypic tetramers.

The constitutive MCs in most connective tissues of the WT BALB/c mouse express mMCP-6 and mMCP-7. However, the corresponding MCs in WT C57BL/6 (B6) mice lack mMCP-7 because of an exon 2/intron 2 splice-site mutation in its gene (4). Using homologous recombination approaches, we created transgenic B6 mouse lines that lack mMCP-6 but express mMCP-7 (designated hereafter as "$6^-/7^+$ B6 mice") or lack both tetramer-forming tryptases (designated hereafter as "$6^-/7^-$ B6 mice") (5, 6). We previously showed that mMCP-6–deficient animals were unable to combat bacterial and helminth infections efficiently relative to WT B6 ($6^+/7^-$) and WT BALB/c ($6^+/7^+$) mice. The mechanisms by which mMCP-6 plays beneficial roles in innate immunity have not been elucidated at the molecular level, but neutrophil recruitment was significantly delayed in *Klebsiella pneumoniae*-infected $6^-/7^-$ B6 mice. Neutrophils are bactericidal, and a failure to recruit peripheral blood neutrophils rapidly into the infected tissues of these animals correlated with increased circulating and tissue bacterial loads (5). The human ortholog of mMCP-6 is human tryptase-β (hTryptase-β) (7, 8). In support of the data obtained from MC- and mMCP-6–deficient mice, the administration of 2–10 μg of recombinant mMCP-6 (9) or hTryptase-β (10) into the mouse's peritoneal cavity or lung, respectively, resulted in a prominent neutrophilia. The latter hTryptase-β–treated W/W^v mice also were able to combat a pulmonary *K. pneumoniae* infection effectively (10).

Contrary to the beneficial roles of MCs in bacterial and helminth infections, numerous studies have documented detrimental roles for MC-restricted proteases in inflammatory disorders. For example, we showed that experimental inflammatory arthritis was significantly attenuated in $6^-/7^-$ B6 mice and $6^-/7^+$ B6 mice relative to $6^+/7^-$ B6 mice (11, 12). Increased numbers of hTryptase-β^+ MCs have been detected in intestinal specimens from patients with ulcerative colitis (UC) and Crohn disease (13). Colorectal biopsies from UC patients also constitutively released significantly more immunoreactive hTryptase-β into the conditioned medium than did colorectal biopsies from normal individuals (14). Nevertheless, it remains to be determined if MC-restricted tryptases have prominent proinflammatory activities in inflammatory bowel disease (IBD).

Oral administration of dextran sodium sulfate (DSS) (15, 16) or rectal administration of trinitrobenzene sulfonic acid (TNBS) (17) results in acute colitis in rodents that resembles aspects of IBD. In the DSS model, damage to the epithelium results in increased mucosal permeability, allowing gut flora and exogenous antigens better access to the colon's mucosal and submucosal layers (18, 19). Activation of poorly defined immune pathways ultimately results in the extravasation of large numbers of peripheral blood neutrophils and other inflammatory cells into the colon, loss of epithelial cells and goblet cells, and proteolytic damage to the colon's ECM. In the TNBS model, breakdown of the epithelial by alcohol and subsequent haptenization of colonic proteins by TNBS results in transmural inflammation in the colon (20). The DSS- and TNBS-induced colitis models therefore have given valuable insight as to the importance of colonic epithelial barrier function and the acute inflammatory response to injury and lu-

Author contributions: M.J.H., M.J.S., G.D.L., S.A.K., R.S.B., R.A., D.M.L., and R.L.S. designed research; M.J.H., M.J.S., G.D.L., J.N.G., X.W., W.X., and R.L.S. performed research; G.D.L., D.M.L., and R.L.S. contributed new reagents/analytic tools; M.J.H., M.J.S., G.D.L., J.N.G., W.X., S.A.K., R.S.B., R.A., D.M.L., and R.L.S. analyzed data; and M.J.H., M.J.S., R.S.B., R.A., D.M.L., and R.L.S. wrote the paper.

Conflict of interest statement: G.D.L. is an employee of Biomodels, LLC. This company did not fund the study, and the other authors have no affiliation with the company.

This article is a PNAS Direct Submission. W.S. is a guest editor invited by the Editorial Board.

[1]To whom correspondence should be addressed. E-mail: mjhamilton@partners.org.

This article contains supporting information online at www.pnas.org/lookup/suppl/doi:10.1073/pnas.1005758108/-/DCSupplemental.

minal antigens in the lower gastrointestinal tract. We now show that MCs, and more specifically their tryptase mediator mMCP-6 (but not mMCP-7), play an essential role in chemically induced experimental colitis.

Results

Identification of mMCP-6–Expressing MCs in the Mouse Colon. We previously showed that the heparin-positive MCs that reside in the serosal and submucosal regions of the mouse's jejunum of all examined mouse strains constitutively express mMCP-6 (21). It has not been shown to date whether the MCs in the mouse colon express this tryptase. As noted in Fig. 1, MCs could be identified in the mucosal, submucosal, and serosal regions of the colons of WT B6 mice that contained mMCP-6 protein as assessed by immunohistochemistry. In support of these data, the mMCP-6 transcript was detected in replicate colon samples by real-time PCR analysis.

Weight Loss, Histochemistry, and Endoscopy Scores of DSS-treated WT $6^+/7^-$ and Transgenic $6^-/7^-$ B6 Mice. Many studies have shown that WT mice that have received DSS in their drinking water develop catabolic wasting. We therefore measured the degree of weight loss in $6^+/7^-$ and $6^-/7^-$ B6 mice throughout our 9-d DSS experiments. In three separate experiments (Fig. 2*A*), DSS-treated $6^+/7^-$ B6 mice ($n = 26$) lost 7.0 ± 1.0% of their body mass, and $6^-/7^-$ B6 mice ($n = 27$) lost 0.2 ± 1.0% ($P < 0.0001$) of their body mass, whereas untreated mice gained a small amount of weight during the course of the experiment. To assess microscopic changes in experimental colitis that correlate with these weight changes, a 20-point scoring system (22) was used based on six different categories of mucosal damage and inflammation. In two examined DSS experiments (Fig. 2*B*), there was a significant difference in the histopathology scores between the B6 mouse strains that varied in their expression of mMCP-6. DSS-treated $6^+/7^-$ mice ($n = 15$) developed more severe inflammation (score 12.3 ± 0.7) than $6^-/7^-$ mice ($n = 15$) (score 5.0 ± 1.0; $P < 0.0001$). Representative images highlight the extensive pathology seen in DSS-treated $6^+/7^-$ mice with the characteristic ulceration, crypt loss, goblet cell loss, and inflammatory cell infiltrate (Figs. 3 *A–E*). The amount of inflammation in DSS-treated $6^-/7^-$ B6 mice (Fig. 3*D*) often was indistinguishable from that in untreated $6^+/7^-$ B6 mice (Fig. 3*E*). Likewise, the mucosal architecture of the colon was rarely perturbed.

To evaluate the composition of the inflammatory infiltrate, the numbers of neutrophils were enumerated in the distal half of the colons of mice from one of the representative DSS experiments. As previously found by others (23), there was a significant increase in the number of neutrophils per high-power field (31.4 ± 4.1) in the colons of our DSS-treated $6^+/7^-$ mice (Figs. 3 *B*, *C*, and *F*) than in the colons of untreated mice, where neutrophils were scarce. In agreement with the pathology scores, DSS-treated

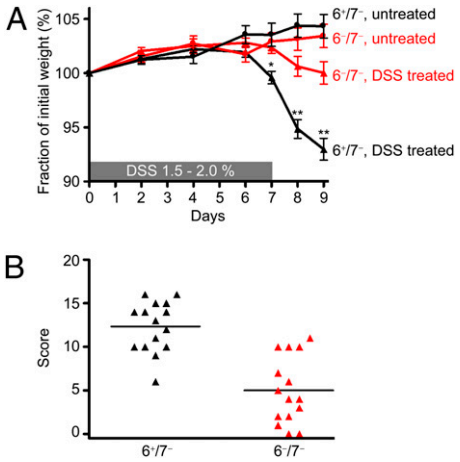

Fig. 2. The $6^-/7^-$ B6 mice are protected from DSS-induced colitis. (*A*) DSS-treated $6^-/7^-$ mice lost significantly less of their initial body weight than similarly treated $6^+/7^-$ mice. Weight loss scores are reported as mean ± SEM. $*P = 0.0014$; $**P < 0.0001$. (*B*) Using a 20-point scoring system, we found DSS-treated $6^-/7^-$ B6 mice also had significantly lower histopathology scores than the DSS-treated $6^+/7^-$ mice. Data are presented in a scatter plot.

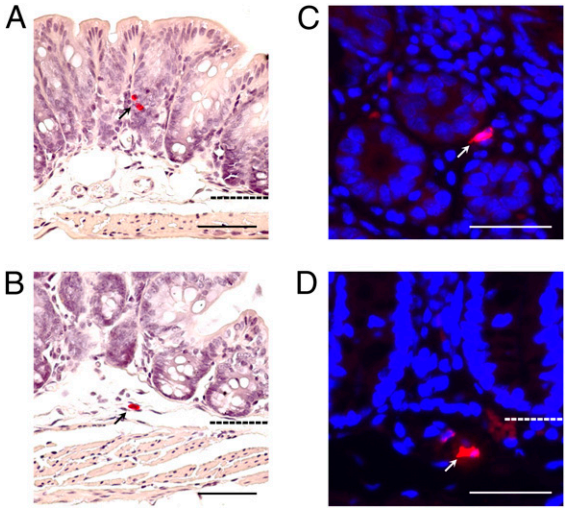

Fig. 1. mMCP-6^+ MCs are present in the normal adult mouse colon. (*A* and *B*) Chloroacetate esterase histochemistry was used to identify MCs in colonic tissue sections from normal adult B6 mouse colon. Positive cells (red, marked with black arrows) were detected in the mucosal (*A*) and submucosal (*B*) layers. Dashed lines indicate layer boundaries. (*C* and *D*) Fluorescent immunohistochemistry was used to visualize mMCP-6^+ MCs in the colon. mMCP-6^+ MCs (red cells indicated by white arrows) were observed in the mucosa (*C*), submucosa (*D*), and serosa (not shown). (Scale bars: 50 μm.)

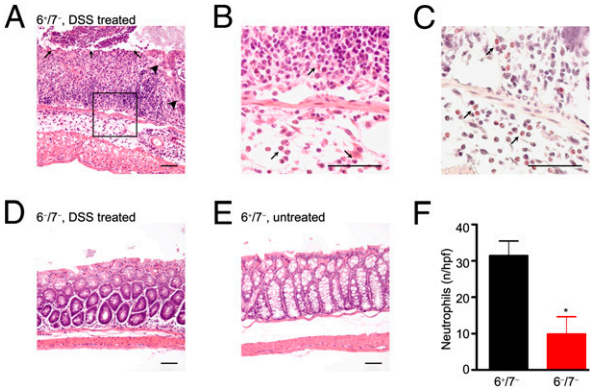

Fig. 3. DSS-induced colitis histopathology is less severe in $6^-/7^-$ mice than in $6^+/7^-$ mice. (*A–E*) The colons of the DSS-treated and untreated $6^+/7^-$ and $6^-/7^-$ mice were harvested, fixed, and stained. (*A*) Severe inflammation, in particular ulceration (black arrows), loss of crypts (large black arrowheads), and increased inflammatory infiltrate can be seen in the representative colon from a DSS-treated $6^+/7^-$ mouse. The majority of the infiltrating inflammatory cells are neutrophils, as assessed at higher power by H&E staining (black arrows in *B*) and by chloroacetate esterase histochemistry (pink-staining cells indicated by black arrows) (*C*). In contrast, the histopathology of the colon of the DSS-treated $6^-/7^-$ mouse in *D* resembles that of the untreated $6^+/7^-$ mouse in *E*. (Scale bars: 50 μm.) (*F*) There are significant differences in the numbers of neutrophils per high-power field (mean ± SEM) in the colon segments of DSS-treated $6^+/7^-$ and $6^-/7^-$ mice. $*P = 0.007$.

IMMUNOLOGY

$6^-/7^-$ B6 mice had significantly fewer colonic neutrophils (9.8 ± 4.8; $P = 0.007$) than similarly treated WT mice (Fig. 3*F*). There did not appear to be an overall difference in the distribution of the neutrophils, which in $6^-/7^-$ B6 mice continued to be located at sites of ulceration and/or crypt loss in the colon mucosa and submucosa. The locations and numbers of neutrophils were confirmed by immunohistochemical staining using an anti-neutrophil antibody. As assessed by H&E and Congo red staining, eosinophils were rare in all examined colons of DSS-treated mice.

We next evaluated gross mucosal changes in the colons of living mice at various time points of the DSS protocol using endoscopy (Fig. 4 and Movies S1, S2, and S3). In these experiments, the degree of colitis was scored by a blinded investigator (G.D.L) on a 0–4 scale on days 7, 9, and 14 and then was averaged between two DSS experiments. The scoring scale assigns a score based upon various criteria ranging from normal (score = 0), apparent loss of vascularity (score = 1), presence of contact bleeding (score = 2), presence of erosions (score = 3), and ulcerations (score = 4). In agreement with our histopathology data (Fig. 3), $6^+/7^-$ B6 mice ($n = 32$) had significantly higher endoscopy scores at day 9 (2.1 ± 0.1), suggesting more colonic inflammation, than did $6^-/7^-$ B6 mice ($n = 32$, 1.1 ± 0.2; $P < 0.0001$) (Fig. 4). Among the DSS-treated mice, 16% (5/32) of the 32 $6^-/7^-$ B6 mice, but none of the $6^+/7^-$ B6 mice, were endoscopically normal and received a score of 0. The overall difference in inflammatory scores persisted through day 14 (Fig. 4*B*). The TNBS model was used to confirm the importance of mMCP-6 in experimental colitis. Because of the correlation between endoscopy scores and histopathology severity in the DSS model, endoscopy was used again to evaluate the degree of colon inflammation in mice differing in expression of mMCP-6. In two averaged experiments and in agreement with the DSS data, TNBS-treated $6^+/7^-$ B6 mice ($n = 18$) had significantly higher endoscopy scores at day 3 (2.8 ± 0.2) and day 5 (2.6 ± 0.2) (Movie S4) than did similarly treated $6^-/7^-$ B6 mice ($n = 19$) at day 3 (1.9 ± 0.1; $P < 0.0001$) and day 5 (1.6 ± 0.1; $P < 0.0001$) (Fig. S1 and Movie S5).

Confirmation That mMCP-6 Is an Essential MC-Derived Mediator in DSS-Induced Colitis. To verify that mMCP-6 is a critical proinflammatory mediator in DSS-induced colitis and to evaluate the importance of the related tryptase mMCP-7 in this disease model, we next evaluated the DSS susceptibility of a second B6 mouse strain we created that lacks mMCP-6 but expresses mMCP-7. In two separate experiments (Fig. 5*A*), DSS-treated $6^-/7^+$ B6 mice ($n = 11$) did not lose weight by the end of the experiment (+0.9 ± 1.2%) compared with treated WT $6^+/7^-$ mice ($n = 12$, −9.3 ± 2.0%; $P = 0.0005$). Like the DSS-treated $6^-/7^-$ B6 mice, DSS-treated $6^-/7^+$ B6 mice also had reduced histopathology scores relative to WT control mice (5.1 ± 0.6 vs. 11.5 ± 0.9; $P < 0.0001$) (Fig. 5*B*).

Another major serine protease present in the mMCP-6^+ MCs that reside in most tissues is mMCP-5. We discovered that the MCs in the colons of WT B6 mice also express mMCP-5 as assessed by real-time PCR. To determine the possible role of this MC-restricted serine protease in colitis, we evaluated the responses of our mMCP-5–null B6 mice to the DSS protocol. In two separate DSS experiments, mMCP-5–null B6 mice ($n = 12$) were found to be indistinguishable from that of WT mice ($n = 12$) at day 9 in terms of weight loss (Fig. 5*C*) and histopathology scores (Fig. 5*D*).

Expression of Mediators in Colon Segments of Untreated and DSS-Treated B6 Mice. To begin to understand mechanistically how mMCP-6 might contribute to inflammation, epithelial cell loss, and proteolytic damage of the colon's ECM in the DSS model of experimental colitis, the levels of the transcripts that encode essentially every known mouse protein were quantitated by microarray analysis. For these experiments, RNA was isolated from distal colon segments at day 9. Noted in Dataset S1 are the complete microarray data of three colon RNA samples isolated from a nontreated $6^+/7^-$ B6 mouse, a DSS-treated $6^+/7^-$ B6 mouse, and a DSS-treated $6^-/7^-$ B6 mouse. Several differentially expressed transcripts identified by microarray analysis were selected for confirmatory analysis because of their perceived significance in humans with IBD. In these experiments, RNA was isolated from untreated and DSS-treated $6^+/7^-$ and $6^-/7^-$ mice (six to eight mice per group in two independent experiments), and the expression of the selected transcripts was determined by real-time PCR. The results in each group were averaged and then expressed as fold-change differences relative to untreated $6^+/7^-$ mice. As reported by others (24), we found that the transcripts that encode the proinflammatory cytokines IL-1β and IL-6 were increased markedly in the colons of DSS-treated $6^+/7^-$ mice (Fig. 6), in agreement with our microarray data (Dataset S1). Although the levels of the IL-1β transcript in the colon segments of DSS-treated WT mice were increased by ∼100-fold compared with levels in untreated mice, there was only a fourfold increase in the expression of this proinflammatory cytokine in the corresponding tissue samples from DSS-treated $6^-/7^-$ mice. To extend our mRNA data, we quantified the levels of these proinflammatory cytokines in distal colon segments by ELISA. In support of our microarray (Dataset S1) and real-time PCR data (Fig. 6), the levels of IL-6 protein in the conditioned

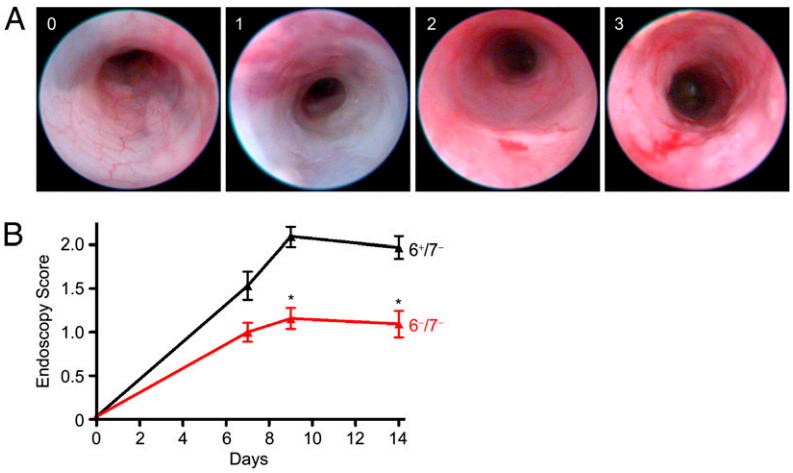

Fig. 4. DSS-treated $6^-/7^-$ mice have a more benign endoscopic appearance than DSS-treated $6^+/7^-$ mice. (*A*) Representative images from the endoscopy grading scale for the scores 0, 1, 2, and 3. Note the apparent loss of vascularity with a score of 1, the appearance of contact bleeding with a score of 2, and the mucosal erosions in a mouse with a score of 3. (*B*) Inflammation was quantitated using the endoscopy scale at days 7, 9, and 14. In agreement with the histopathology data, DSS-treated $6^-/7^-$ mice had significantly lower endoscopy scores at days 9 and 14 than DSS-treated $6^+/7^-$ mice. Endoscopy scores are reported as mean ± SEM. *$P < 0.0001$.

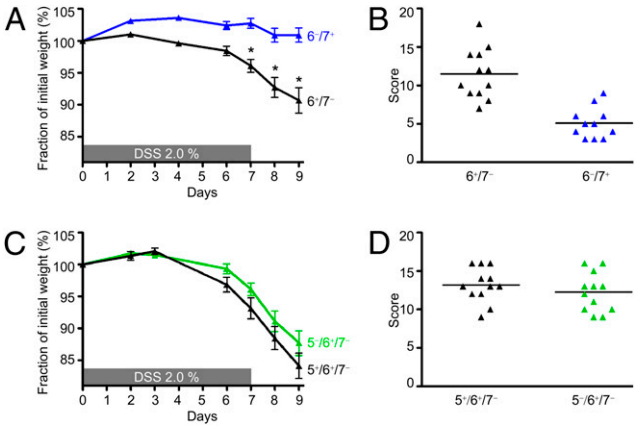

Fig. 5. mMCP-6–null $6^{-}/7^{+}$ B6 mice resemble mMCP-6–null $6^{-}/7^{-}$ B6 mice in the DSS-induced colitis model, whereas mMCP-5–null B6 mice resemble WT B6 mice. (*A* and *B*) In two experiments, DSS-treated $6^{-}/7^{+}$ B6 mice displayed significantly less weight loss (*A*) and histopathology scores (*B*) than similarly treated $6^{+}/7^{-}$ B6 mice. Weight loss scores are reported as mean ± SEM. $^{*}P < 0.0005$. Histopathology data are presented in a scatter plot. (*C* and *D*) DSS-treated mMCP-5–null B6 mice displayed weight loss (*C*) and histopathology scores (*D*) similar to those of DSS-treated $6^{+}/7^{-}$ B6 mice. Weight loss scores are reported as mean ± SEM. Histopathology data are presented in a scatter plot.

media of colon samples from DSS-treated $6^{+}/7^{-}$ and $6^{-}/7^{-}$ mice were 488 pg/mL ± 163 and 126 pg/mL ± 42, respectively ($n = 10$ for each group; $P = 0.046$). The levels of IL-1β protein from homogenized distal colon segments were 168 ± 28 pg/mL and 65 ± 11 pg/mL, respectively ($n = 10$ for each group; $P = 0.003$).

We previously showed that mMCP-6 is necessary for efficient neutrophil recruitment into tissues in experimental arthritis and bacterial infections. This MC-restricted tetramer-forming tryptase probably exerts its proinflammatory effects, in part, by inducing bystander cells in tissues to increase their expression of chemokines that are recognized by neutrophils. In our DSS microarray experiment, the levels of the transcripts that encode chemokine (C-X-C motif) ligands 1 (CXCL1) and 2 (CXCL2) and many other chemokines were much more abundant in the colons of DSS-treated $6^{+}/7^{-}$ mice than in the colons of untreated $6^{+}/7^{-}$ mice and DSS-treated $6^{-}/7^{-}$ mice (Dataset S1). In our follow-up real-time PCR experiments that evaluated CXCL1 mRNA levels in the colons of eight different mice in each group, there was a mean sevenfold increase in the expression of this neutrophil-responsive chemokine in DSS-treated $6^{+}/7^{-}$ mice relative to that in untreated WT mice and DSS-treated $6^{-}/7^{-}$ mice (Fig. 6).

In our microarray analysis, we discovered that several matrix metalloproteinases (MMPs) important in ECM remodeling (e.g., MMP3, MMP9, and MMP13) also were markedly increased in the colonic segments of DSS-treated WT mice relative to untreated WT mice and DSS-treated $6^{-}/7^{-}$ mice (Dataset S1). From the real-time PCR data (Fig. 6), the transcripts that encode MMP3 and MMP13 were induced at levels 18- and 65-fold higher, respectively, than in untreated WT mice, but in MC-tryptase–null mice these MMPs were induced at levels only 2.6- and 1.5-fold higher, respectively. We used immunohistochemistry to evaluate MMP3 protein expression in the DSS-treated mice. In agreement with the mRNA data, MMP3 staining in the colons of DSS-treated $6^{+}/7^{-}$ mice was increased relative to DSS-treated $6^{-}/7^{-}$ mice and untreated $6^{+}/7^{-}$ mice (Fig. 7).

In addition to the transcripts that were induced by DSS in WT mice, a number of constitutively abundant transcripts in the colonic segments of untreated B6 mice were decreased substantially in DSS-treated $6^{+}/7^{-}$ B6 mice but not in DSS-treated $6^{-}/7^{-}$ B6 mice (Fig. 6 and Dataset S1). For example, the levels of the transcript that encodes solute carrier family 26 member 3 (SLC26A3) decreased by 19.3 ± 6.2-fold and 5.3 ± 1.0-fold in DSS-treated $6^{+}/7^{-}$ and $6^{-}/7^{-}$ B6 mice, respectively ($n = 6$ in each instance), relative to untreated WT $6^{+}/7^{-}$ B6 mice. Immunohistochemical analysis of resected colon specimens confirmed fewer $SLC26A3^{+}$ cells in DSS-treated $6^{+}/7^{-}$ mice than in DSS-treated $6^{-}/7^{-}$ mice and untreated $6^{+}/7^{-}$ mice (Fig. 7).

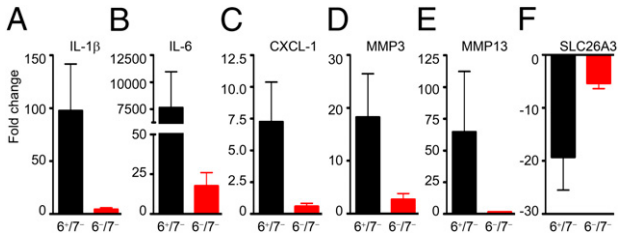

Fig. 6. Levels of the transcripts that encode numerous chemokines, cytokines, and MMPs are reduced in the colons of DSS-treated $6^{-}/7^{-}$ B6 mice. Microarray and real-time PCR assays were performed on RNA isolated from the distal colons of untreated and DSS-treated $6^{+}/7^{-}$ and $6^{-}/7^{-}$ mice to identify transcripts that are expressed differentially in this colitis model at day 9. The resulting GeneChip data (Dataset S1) revealed that many chemokines, cytokines, MMPs, and other proteins that have been implicated by others in patients with IBD were differentially expressed at the RNA level. To confirm and extend these microarray data, real-time PCR approaches were used to compare the levels of the transcripts that encode CXCL1, IL-1β, MMP3, MMP13, IL-6, and SLC26A3 in RNA samples from larger numbers of untreated and DSS-treated $6^{+}/7^{-}$ and $6^{-}/7^{-}$ mice. Data are expressed as the fold change (mean ± SEM) in these groups of mice relative to the untreated $6^{+}/7^{-}$ B6 mice.

Discussion

Current therapies used to treat IBD are limited in efficacy because of an incomplete understanding of the individual differences in disease pathogenesis that exist among individual patients. Most experts agree that IBD is a consequence of abnormal immune responses to intestinal lumen pathogens and exogenous antigens (25). Because increased numbers of activated and degranulating MCs have been found in IBD patients (26, 27), we hypothesized that MCs and one or more of their granule protease mediators

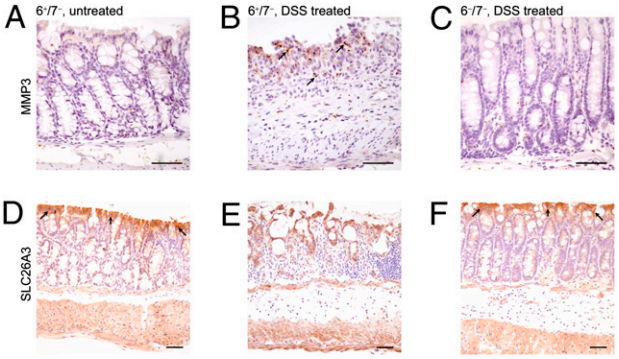

Fig. 7. MMP3 and SLC26A3 protein levels in DSS-treated $6^{-}/7^{-}$ mice relative to DSS-treated $6^{+}/7^{-}$ mice. (*A–C*) MMP3 protein levels were assessed by immunohistochemistry. As shown in *A*, there is minimal MMP3 staining in the colonic mucosa and submucosa of untreated WT mice. However, the inflamed mucosal and submucosal layers of DSS-treated $6^{+}/7^{-}$ mice (black arrows in *B*) have increased staining, corresponding to MMP3, in contrast to the DSS-treated $6^{-}/7^{-}$ mice (*C*) that resemble the untreated WT mice. (*D–F*) The same representative mouse groups demonstrating staining for SLC26A3. In agreement with the RNA data, there is decreased expression of SLC26A3 in the DSS-treated $6^{+}/7^{-}$ mice (*E*) compared with WT untreated mice (black arrows in *D*) and DSS-treated $6^{-}/7^{-}$ mice (black arrows in *F*). (Scale bars: 50 μm.)

might have a significant role in animal models that simulate various aspects of colitis in IBD.

In our present study, we show that the MCs in the colons of WT B6 mice express mMCP-6 (Fig. 1) and that this tetramer-forming tryptase is essential in the DSS experimental model of colitis (Figs. 2–7, Dataset S1, and Movies S1, S2, and S3). DSS-treated $6^-/7^+$ B6 mice (Fig. 5) and $6^-/7^-$ B6 mice (Fig. 2) lost distinctly less weight and had reduced histopathology scores (Figs. 2, 3, and 5) and endoscopy scores (Fig. 4) than similarly treated $6^+/7^-$ B6 mice. This difference in colitis severity was confirmed endoscopically in a second model when $6^+/7^-$ and $6^-/7^-$ B6 mice were exposed to TNBS (Fig. S1 and Movies S4 and S5). In support of our data, others have reported that 27 of the 56 UC patients that received the tryptase inhibitor APC-2059 improved clinically (28) and that the tryptase/kallikrein inhibitor nafamostat mesilate decreased mucosal inflammation in TNBS-treated rats (29).

The expression of numerous cytokines, chemokines, MMPs, and other biologically active factors were significantly reduced in the colons of DSS-treated $6^-/7^-$ B6 mice (Figs. 6 and 7 and Dataset S1). Although mMCP-6 and mMCP-7 are closely related and can have redundant proinflammatory activities in some disease states (11), the substrate preferences of the two tryptases are not identical (9, 30). The observation that substantial pathology occurs in DSS-treated $6^+/7^-$ B6 mice, but in not $6^-/7^+$ and $6^-/7^-$ mice (Figs. 2–5), allowed us to conclude that the most important tryptase in our experimental colitis studies is mMCP-6, the putative mouse ortholog of hTryptase-β. Although there are no comparative studies of MC tryptase in intestinal inflammation, our results are in agreement with those noted in our earlier studies of inflammatory arthritis (11, 12).

Another major serine protease present in the mMCP-6^+ population of MCs in the colon is the chromosome 14C3 family member mMCP-5 (31). Although mMCP-5 is a member of the chymase family whose amino acid sequence is most similar to that of human chymase-1, mMCP-5 has elastase-like activity (32). Ishida and colleagues (33) noted that the histopathology was significantly reduced in WT BALB/c mice given the chymase inhibitor NK3201 followed by a relatively high concentration of DSS in their drinking water. DSS-induced colitis was not significantly reduced in our DSS-treated mMCP-5–null B6 mice (Fig. 5). These data suggest that another chymase family member (e.g., mMCP-4) has a more prominent role than mMCP-5 in the colitis model. Alternately, there is chymase/elastase-like redundancy in DSS-induced colitis in the mouse, analogous to the tryptase redundancy found in methylated BSA-induced arthritis (11). It also is possible that chymase/elastase-like MC mediators do not play significant roles in acute experimental colitis.

We found that DSS-treated $6^-/7^+$ and $6^-/7^-$ B6 mice had considerably fewer colonic neutrophils than did similarly treated $6^+/7^-$ B6 mice (Fig. 3). We previously showed that recombinant mMCP-6 and its human homolog hTryptase-β can induce cultured endothelial cells and mesenchymal cells to increase their expression of neutrophil-responsive CXCL chemokines. The accumulated data suggest that, in the DSS model, MC-derived tetramer-forming tryptases promote neutrophil accumulation in the colon in an indirect manner. The increased expression of several chemokines in our microarray (Dataset S1) and real-time PCR analyses (Fig. 6) of DSS-treated $6^+/7^-$ mice relative to similarly treated $6^-/7^-$ mice support this possibility.

Our histopathology data (Fig. 3) also suggest that mMCP-6 plays a key role in the chemically induced loss of epithelial cells and ECM from the colon. In agreement with these data, the transcripts that encode several MMPs important in ECM remodeling (e.g., MMP3 and MMP13) were significantly increased at day 9 in the colons of DSS-treated $6^+/7^-$ B6 mice relative to $6^-/7^-$ B6 mice (Dataset S1 and Figs. 6 and 7).

We also were able to identify several constitutively expressed proteins in the colon whose expression was markedly down-regulated in the DSS animal model of colitis (Dataset S1). We focused on the transcript that encodes the chloride ion-channel protein SLC26A3 because a single nucleotide polymorphism that resides within this gene's promoter was linked recently to UC (34). As noted in Dataset S1 and Figs. 6 and 7, the dampened expression of SLC26A3 in DSS-induced colitis confirms a central and early role for mMCP-6 in different pathways in experimental colitis.

In summary, we have shown that mMCP-6 has prominent proinflammatory roles in DSS- and TNBS-induced colitis, and we obtained insight as to how this MC-restricted tryptase mechanistically controls the inflammation and damage to the colon's ECM. It therefore is conceivable that the development of the next generation of tryptase inhibitors that are more specific to hTryptase-β will have beneficial value in the therapy of patients with IBD.

Materials and Methods

Mice. WT ($6^+/7^-$) B6 mice were obtained from Taconic. As previously described, transgenic $6^-/7^-$ B6 mice (5) were created using a homologous recombination approach, whereas transgenic $6^-/7^+$ B6 mice (6) were created using a KO/knock-in homologous recombination approach. The mMCP-5–null ($5^-/6^+/7^-$) B6 mice were generated in 129/Sv mouse embryonic stem cells, and the resulting mice were backcrossed 10 generations onto the B6 mouse strain. All animals were housed at Taconic's isolated barrier animal facility in Germantown, NY. Mice were transported to the animal facilities at Biomodels LLC (Watertown, MA) and Brigham and Women's Hospital (BWH)/Dana Farber Cancer Institute (DFCI). They were allowed to acclimate for at least 1 wk before any experiment. Mice were maintained on LabDiet 5001 (Purina) and water. Animals were age (8–10 wk) and gender matched in each experiment. All animal studies were carried out using protocols approved by the BWH/DFCI and Biomodels Institutional Animal Care and Use Committees.

DSS- and TNBS-induced Colitis. Mice were exposed to 36–50 kDa DSS (MP Biomedicals) at a concentration of 1.5–2.0% in their drinking water for 7 d, as previously described (15). Preliminary studies using 8-wk-old male WT B6 mice revealed that exposure to DSS in the water for 7 d caused a 7–17% weight loss in WT mice with minimal mortality and maximal inflammation as measured by histology at day 9. Mice therefore routinely received an additional 2 d of regular drinking water before they were killed at day 9. Colons then were harvested for histopathology, RNA isolation, and protein assays (*SI Experimental Procedures*). In the endoscopy experiments, mice received an additional 7 d of regular drinking water before their final analysis at day 14. In the TNBS experiments, colitis was induced by intrarectal administration of 4 mg/100 μL TNBS (Sigma) in 50% ethanol under isoflurane anesthesia on day 0. Mice received regular drinking water and chow throughout the experiment and were killed on day 5.

Mouse Endoscopy. WT $6^+/7^-$ and transgenic $6^-/7^-$ B6 animals were sent to Biomodels LLC for endoscopic examination. After a 1-wk acclimation period, mice were treated with DSS or TNBS using the above protocols. On days 0, 7, 9, and 14 for the DSS-treated mice and on days 0, 3, and 5 for the TNBS-treated mice, the animals were anesthetized with isoflurane, and the distal two-thirds of the colons were examined using a small-animal video endoscope (Karl Storz). The degree of colon inflammation was scored by a blinded investigator using a four-point scale developed by Biomodels LLC for experimental colitis. Pictures and movies were taken of representative mice using the associated imaging equipment.

RNA Isolation from Mouse Colon and Evaluation of Transcript Expression by Microarray and Real-Time PCR Approaches. On day 9 of an individual DSS experiment, ~1-cm sections of distal colons were resected and placed into RNAlater (Ambion) at 4 °C overnight. Tissue samples were washed in PBS, and RNA was purified using a homogenizer and RNeasy columns (Qiagen). To evaluate global changes in transcript expression as a result of DSS administration, RNA was isolated from the colons of DSS-treated $6^+/7^-$ and $6^-/7^-$ B6 mice and was compared with RNA isolated from the colons of untreated $6^+/7^-$ B6 mice by microarray analyses using Affymetrix 430_2.0 mouse GeneChips. RNA amplification, labeling, and hybridization were performed by the DFCI Microarray Core Facility. (The complete protocol is available at http://chip.dfci.harvard.edu.) To confirm some of the microarray findings, cDNA was synthesized from RNA from six to eight mice per group

and analyzed by real-time PCR using Qiagen's validated primers. Results for each transcript were tabulated using the standard curve method and were normalized based on the level of the GAPDH transcript in each sample. The data obtained are presented as fold-change differences of the DSS-treated strains of mice compared with the non–DSS-treated WT controls.

Statistical Analysis. Data were analyzed using GraphPad Prism software version 4.00. Student's unpaired *t* test was performed to evaluate means ± SE to compare changes in inflammatory cell numbers, weight changes, histological and endoscopic analysis, and real-time PCR and ELISA values. *P* values <0.05 were considered statistically significant.

ACKNOWLEDGMENTS. This work was supported by National Institutes of Health Grants HL036610, AI065858, and AI059746 (all to R.L.S.); DK44319 and DK007533 (both to R.S.B.); a grant from the Australian National Health and Medical Research Council (to S.A.K.); funds from the Harvard Digestive Diseases Center (to R.S.B. and M.J.H.); and by research fellowship grants from the Crohn's and Colitis Foundation of America (to M.J.H.) and the Harvard Club of Australia Foundation (to S.A.K. and R.L.S.).

1. Reynolds DS, et al. (1990) Different mouse mast cell populations express various combinations of at least six distinct mast cell serine proteases. *Proc Natl Acad Sci USA* 87:3230–3234.
2. Reynolds DS, Gurley DS, Austen KF, Serafin WE (1991) Cloning of the cDNA and gene of mouse mast cell protease-6. Transcription by progenitor mast cells and mast cells of the connective tissue subclass. *J Biol Chem* 266:3847–3853.
3. McNeil HP, et al. (1992) Isolation, characterization, and transcription of the gene encoding mouse mast cell protease 7. *Proc Natl Acad Sci USA* 89:11174–11178.
4. Hunt JE, et al. (1996) Natural disruption of the mouse mast cell protease 7 gene in the C57BL/6 mouse. *J Biol Chem* 271:2851–2855.
5. Thakurdas SM, et al. (2007) The mast cell-restricted tryptase mMCP-6 has a critical immunoprotective role in bacterial infections. *J Biol Chem* 282:20809–20815.
6. Shin K, et al. (2008) Mouse mast cell tryptase mMCP-6 is a critical link between adaptive and innate immunity in the chronic phase of *Trichinella spiralis* infection. *J Immunol* 180:4885–4891.
7. Miller JS, Moxley G, Schwartz LB (1990) Cloning and characterization of a second complementary DNA for human tryptase. *J Clin Invest* 86:864–870.
8. Vanderslice P, et al. (1990) Human mast cell tryptase: Multiple cDNAs and genes reveal a multigene serine protease family. *Proc Natl Acad Sci USA* 87:3811–3815.
9. Huang C, et al. (1998) Induction of a selective and persistent extravasation of neutrophils into the peritoneal cavity by tryptase mouse mast cell protease 6. *J Immunol* 160:1910–1919.
10. Huang C, et al. (2001) Evaluation of the substrate specificity of human mast cell tryptase β I and demonstration of its importance in bacterial infections of the lung. *J Biol Chem* 276:26276–26284.
11. McNeil HP, et al. (2008) The mouse mast cell-restricted tetramer-forming tryptases mouse mast cell protease 6 and mouse mast cell protease 7 are critical mediators in inflammatory arthritis. *Arthritis Rheum* 58:2338–2346.
12. Shin K, et al. (2009) Mast cells contribute to autoimmune inflammatory arthritis via their tryptase/heparin complexes. *J Immunol* 182:647–656.
13. Gelbmann CM, et al. (1999) Strictures in Crohn's disease are characterised by an accumulation of mast cells colocalised with laminin but not with fibronectin or vitronectin. *Gut* 45:210–217.
14. Raithel M, et al. (2001) Release of mast cell tryptase from human colorectal mucosa in inflammatory bowel disease. *Scand J Gastroenterol* 36:174–179.
15. Okayasu I, et al. (1990) A novel method in the induction of reliable experimental acute and chronic ulcerative colitis in mice. *Gastroenterology* 98:694–702.
16. Dieleman LA, et al. (1994) Dextran sulfate sodium-induced colitis occurs in severe combined immunodeficient mice. *Gastroenterology* 107:1643–1652.
17. Morris GP, et al. (1989) Hapten-induced model of chronic inflammation and ulceration in the rat colon. *Gastroenterology* 96:795–803.
18. Tlaskalová-Hogenová H, et al. (2005) Involvement of innate immunity in the development of inflammatory and autoimmune diseases. *Ann N Y Acad Sci* 1051: 787–798.
19. Venkatraman A, Ramakrishna BS, Pulimood AB, Patra S, Murthy S (2000) Increased permeability in dextran sulphate colitis in rats: Time course of development and effect of butyrate. *Scand J Gastroenterol* 35:1053–1059.
20. Neurath M, Fuss I, Strober W (2000) TNBS-colitis. *Int Rev Immunol* 19:51–62.
21. Friend DS, et al. (1998) Reversible expression of tryptases and chymases in the jejunal mast cells of mice infected with *Trichinella spiralis J Immunol* 160:5537–5545.
22. Garrett WS, et al. (2007) Communicable ulcerative colitis induced by T-bet deficiency in the innate immune system. *Cell* 131:33–45.
23. Farooq SM, et al. (2009) Therapeutic effect of blocking CXCR2 on neutrophil recruitment and dextran sodium sulfate-induced colitis. *J Pharmacol Exp Ther* 329: 123–129.
24. Alex P, et al. (2009) Distinct cytokine patterns identified from multiplex profiles of murine DSS and TNBS-induced colitis. *Inflamm Bowel Dis* 15:341–352.
25. Kaser A, Zeissig S, Blumberg RS (2010) Inflammatory bowel disease. *Annu Rev Immunol* 28:573–621.
26. Bischoff SC, et al. (1996) Quantitative assessment of intestinal eosinophils and mast cells in inflammatory bowel disease. *Histopathology* 28:1–13.
27. Nishida Y, et al. (2002) Different distribution of mast cells and macrophages in colonic mucosa of patients with collagenous colitis and inflammatory bowel disease. *Hepatogastroenterology* 49:678–682.
28. Tremaine WJ, et al.; AXYS Ulcerative Colitis Study Group (2002) Treatment of mildly to moderately active ulcerative colitis with a tryptase inhibitor (APC 2059): An open-label pilot study. *Aliment Pharmacol Ther* 16:407–413.
29. Isozaki Y, et al. (2006) Anti-tryptase treatment using nafamostat mesilate has a therapeutic effect on experimental colitis. *Scand J Gastroenterol* 41:944–953.
30. Huang C, et al. (1997) The tryptase, mouse mast cell protease 7, exhibits anticoagulant activity in vivo and in vitro due to its ability to degrade fibrinogen in the presence of the diverse array of protease inhibitors in plasma. *J Biol Chem* 272:31885–31893.
31. McNeil HP, Austen KF, Somerville LL, Gurish MF, Stevens RL (1991) Molecular cloning of the mouse mast cell protease-5 gene. A novel secretory granule protease expressed early in the differentiation of serosal mast cells. *J Biol Chem* 266:20316–20322.
32. Kunori Y, et al. (2002) Rodent α-chymases are elastase-like proteases. *Eur J Biochem* 269:5921–5930.
33. Ishida K, et al. (2008) Role of chymase-dependent matrix metalloproteinase-9 activation in mice with dextran sodium sulfate-induced colitis. *J Pharmacol Exp Ther* 324:422–426.
34. Asano K, et al. (2009) A genome-wide association study identifies three new susceptibility loci for ulcerative colitis in the Japanese population. *Nat Genet* 41: 1325–1329.